Received: 26 April 2019 | Revised: 21 October 2019 | Accepted: 11 November 2019

DOI: 10.1002/jrs.5796

RESEARCH ARTICLE

WILEY Journal of RAMAN SPECTROSCOPY

Tracking the fungus-assisted biocorrosion of lead metal by Raman imaging and scanning electron microscopy technique

Yiling Wu[1] | Xiaoqing Shao[1] | Hang Jiao[2] | Xinwei Song[1] | Kun He[2] | Zhen Li[1,3]

[1] College of Resources and Environmental Sciences, Nanjing Agricultural University, Nanjing, China

[2] Petrochina Research Institute of Petroleum Exploration & Development, Beijing, China

[3] Jiangsu Key Laboratory for Organic Waste Utilization, Nanjing Agricultural University, Nanjing, China

Correspondence
Zhen Li, College of Resources and Environmental Sciences, Nanjing Agricultural University, Nanjing, Jiangsu 210095, China.
Email: lizhen@njau.edu.cn

Funding information
Fundamental Research Funds for the Central Universities, Grant/Award Number: No. KYZ201712 KYZ201712; National Key R&D Program of China, Grant/Award Number: No. 2017YFC0503902 2017YFC0503902; Program for Student Innovation Through Research and Training, Grant/Award Numbers: 201910307090P and S20190010

Abstract

Fungi play a significant role in biological corrosion of metal materials. We studied the biocorrosion of lead foils under incubation of *Aspergillus niger* (*A. niger*). Multiple techniques, for example, scanning electron microscopy (SEM), diffuse reflectance infrared Fourier transform spectroscopy (DRIFT), and Raman imaging and scanning electron microscopy (RISE), were applied in this study. SEM confirmed the normal growth of the fungus on Pb foil surface, either above or under the solid medium surface. In addition, SEM-energy dispersive spectrometer confirmed the formation of the secondary Pb mineral particles after incubation, which had variable morphologies. DRIFT was able to show changes of compounds formed on the surface of Pb foils. However, it cannot exactly identify the mineral phase. RISE technology offered both morphological and spectral information of the formed Pb mineral. Three dominant Raman peaks at ~1,440, ~1,480, and ~1,590 cm^{-1} indicated that the secondary mineral was lead oxalate. Raman mapping further demonstrated the distribution of Pb oxalate architecture. This study first applied RISE to investigate the biocorrosion of metals by fungi.

KEYWORDS

Aspergillus niger, DRIFT, lead oxalate, Pb, RISE

1 | INTRODUCTION

Lead (Pb) metal is an important structural and industrial material, which has been applied in the manufacturing of machine, pipeline, and shoots.[1] However, metals, including Pb, are substantially subject to biocorrosion,[2] which consequently transforms the metallic Pb into mobile cations. In addition to the loss of the metallic materials, Pb cations enter the environment at a weathering rate of approximately 1–5% per year,[3] which causes serious environmental risk to soil system.[4] The migration of Pb leachate through the liner material into underlying aquifers has caused major public health concern.[5] Pb has hence been one of the most common hazardous heavy metals.[6]

Microorganisms, for example, bacteria and fungi, are both able to accelerate corrosion of multiple metals.[7] They play critical roles in metal biotransformation.[8] In particular, fungi are geologically active agents and are tightly involved in biogeochemical processes within pedosphere and lithosphere.[9] Fungi are able to accelerate the reaction rate via various ways.[10,11] For example, they can secrete abundant organic acids to attack the material matrices.[9] Meanwhile, chelation of metal

Yiling Wu and and Xiaoqing Shao contributed equally in this work.

cations by organic ligands (e.g., citrate and oxalate) can weaken metal–oxygen bonds in minerals and can increase the solubility of metals.[12] Considering the high fungal biomass (compared with bacteria), they should be addressed in priority regarding the biocorrosion in nature.

Aspergillus niger (*A. niger*), a type of filamentous fungi, has been widely explored in fermentation industry and removal of heavy metals.[13,14] It is the fungus with the recognized ability of organic acid production. *A. niger* can secrete a large amount of organic acids, orexample, oxalic ($K\alpha_1 = 6.5 \times 10^{-2}$), tartaric ($K\alpha_1 = 9.2 \times 10^{-4}$), and citric acids ($K\alpha_1 = 7.4 \times 10^{-4}$).[15,16] Therefore, the oxalic acid, with significantly high ionization constant, dominates the organic acid secretion. The secreted organic acids are able to directly react with Pb^{2+} to form soluble mineral crystals, called Pb oxalate (PbC_2O_4), around both cell walls and external medium during bioremediation.[17] The organic acids can also enhance the dissolution of inorganic phosphates and then react with Pb^{2+} to form stable pyromorphite mineral ($Pb_5[PO_4]_3Cl$). Furthermore, its high tolerance to Pb^{2+} toxicity allows that *A. niger* maintains enough bioactivity under Pb stress.[18] However, the growth of *A. niger* on metallic Pb surface has not been fully elucidated yet.

To track the fungus-assisted biocorrosion of metals, many technologies have been applied. Microscopy, for example, scanning electron microscopy (SEM), can be applied to observe the morphology of secondary substances generated on metal surface. Meanwhile, Raman and infrared (IR) spectroscopy (either spot or mapping analysis) can provide fundamental information of the molecular structure for both organic and inorganic components. However, to evaluate biocorrosion of metals, both morphological and chemical properties are necessary.

Raman imaging and scanning electron microscopy (RISE) was first applied to track the fungus-assisted corrosion on Pb metal foils in this study. In addition, SEM and diffuse reflectance infrared Fourier transform spectroscopy (DRIFT) were also applied and were compared with the RISE results.

2 | MATERIALS AND METHODS

2.1 | Strains and biocorrosion experiments

The filamentous fungus, *A. niger* (CGMCC No. 11544, Nanjing Agricultural University), was isolated from the soybean rhizosphere soil in Nanjing, China.[19] It was previously incubated on potato dextrose agar (PDA) plates at 28°C for 5 days to form sporulation prior to the experiments. We used a sterile loop to inoculate spores to solid PDA medium. Then, Pb foils (1 cm × 0.5 cm × 0.5 mm) were inserted into the six inoculated PDA agar plates. In each plate, six replicates (foils) were inserted and were previously sterilized under ultraviolet light for 3 hr. The incubation was performed at 28°C for 6 days. Then we randomly select one agar plate every day (discarded after analysis). The DRIFT spectra were collected every day on the foils to confirm its weakness in identifying Pb oxalate. One spectrum was randomly selected (other five spectra were applied to confirm the repeatability). Additionally, Pb foil surface was investigated by SEM and RISE after a 6-day incubation.

2.2 | Instrumentation

Field-emission SEM was performed in a Carl Zeiss Supra 55 system with an acceleration voltage of 15 kV. To enhance image quality and minimize charging, samples were coated with gold for 15 nm. The semiquantity analysis was performed by Oxford Aztec X-Max 150 energy dispersive spectrometer for 90 s.

DRIFT was performed on a Nicolet iS5 Fourier-transform IR spectrometer (Thermo Fisher Scientific Inc.) equipped with a diffuse reflectance accessory. The spectral region of 400–1,200 cm^{-1} was recorded with 16 times scans for each sample at a spectral resolution of 4 cm^{-1}. Normalization of the spectra was performed using the Thermo Scientific OMNIC software (Thermo Fisher Scientific Inc., Madison, USA).

RISE system consists of a Wissen schaftliche Instrumente and Technologie GmbH (WITech, Germany) Alpha 300 confocal Raman microscope combined with an SEM (TESCAN-VEGA3). Both SEM and light microscopy modes were applied under RISE. The spectral region of 0–4,500 cm^{-1} was recorded using 488-nm laser (3 mW with 30 × 4-s scans). Smoothing and normalization of the spectra were performed using Wissen schaftliche Instrumente and Technologie GmbH Project 5 software.

3 | RESULTS AND DISCUSSION

3.1 | Observation of Pb foil surfaces by SEM

It showed evident surface corrosion and the formation of secondary Pb minerals after a 6-day incubation under SEM (Figure 1). Pb foils showed distinct morphological contrasts between the regions under and above the PDA medium surface (see Figure 1a). Above the medium, the hyphae grew upward and were tightly adhered to the surface of Pb foils (Figure 1b).

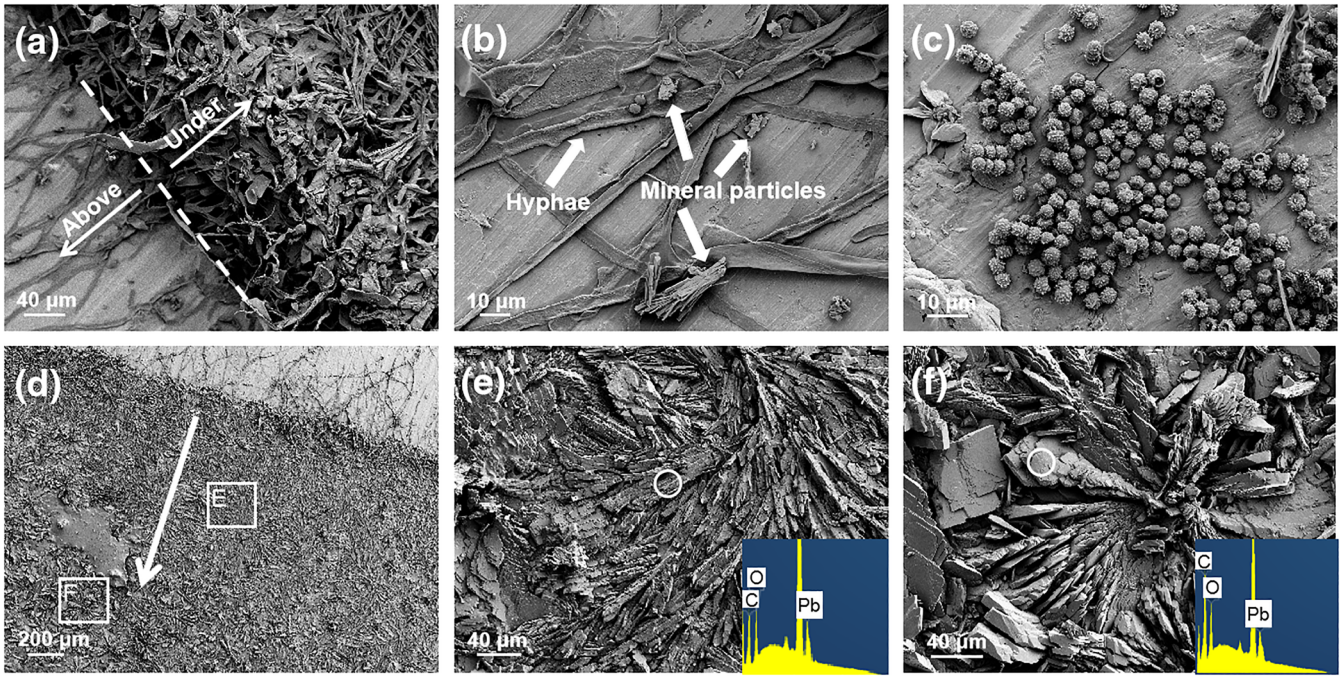

FIGURE 1 SEM imaging on the Pb foil surface after six-days incubation with *A. niger*. A: The distinct surface morphology above the medium and under the medium; B: Hyphae were tightly adhered to the surface of Pb foils above the medium; C: Spores congregated on the surface of Pb foil; D: The sizes of mineral particles increased along the arrow within the culture medium; E and F: The images of the small (E) and large (F) particles from the corresponding boxed areas in image D.

Clusters of spores were observed on the surface of Pb foils, indicating that the fungus had the ability to reproduce normally on Pb foils (Figure 1c). Spores can lead to the Pb materials suffering continuous biocorrosion in the long term. Such high tolerance to Pb causes the extended ability of *A. niger* to corrode Pb. Therefore, the fungus should be critical in Pb metal erosion. Furthermore, it is commonly accepted that toxic metals, at some range of concentrations, can even have positive influences on microbial activity.[20] For example, excessive Pb concentration can even stimulate the bioactivity of *A. niger*, which is substantiated by its respiration. Some fungal functions of corroding Pb metal, for example, the production of oxalic acid, would hence be further enhanced.[18]

Fungi produced more abundant organic acids beneath the medium surface and hence formed denser secondary Pb minerals (Figure 1d). Fungus is critical in enhancing electron transfer of metallic Pb.[5] Moreover, compared with other fungi such as *Penicillium oxalicum*, *A. niger* secretes 40% more organic acids.[21] *A. niger* hence has strong ability to mediate the production of secondary Pb minerals in the presence of metallic Pb. Raman and SEM all confirmed the abundant oxalic acid secretion from *A. niger*. In addition, oxalic acid dominates the acidity (from the fungi) due to its high concentration and high acidity constant ($K\alpha_1 = 6.5 \times 10^{-2}$); thus, the secretion of oxalic acid leads to pH as low as 1–2. In contrast, pH of the acid rain (the natural weathering pathway) is usually around 5–6.[22] Therefore, oxalic acid is a relatively strong acid and of central significance to its chemical properties. The ability of oxalate anions to complex metals results in precipitation of insoluble metal oxalates.[23] They react with Pb cations and cause the formation of Pb oxalates with a relatively low solubility product constant (Ksp) value (10^{-9} to 10^{-11}) on the basis of Equations (1) and (2).[24]

$$Pb = Pb^{2+} + 2e^{-}. \quad (1)$$

$$Pb^{2+} + C_2O_4{}^{2-} = PbC_2O_4. \quad (2)$$

Our previous X-ray diffraction analysis on the similar system (incubation of Pb^{2+} and *A. niger*) also indicated that the dominant mineral phase is Pb oxalate.[19] The incorporation of toxic metals into oxalate minerals may potentially provide a mechanism whereby oxalate-producing fungi can tolerate environments with high concentrations of these toxic metals.[25–27]

The sizes of the mineral particles were enlarged as the depth increased (Figure 1e,f). The elemental composition of these particles indicated the abundance of Pb, confirmed by SEM-energy dispersive spectrometer. The morphology of the secondary Pb minerals is scale like, in contrast to the tetragonal crystals formed after reaction between Pb cations and organic acids in solution.[23,28] Furthermore, the mineral particles were well organized (rather than randomly distributed) as shown in Figure 1

e. This is analogous to the morphology of linear hyphae. It hence implied evident microbial regulation on biomineralization.[18]

3.2 | DRIFT analyses on Pb foils surfaces

DRIFT spectra showed the chemical changes on the surface of Pb foils (Figure 2). The peak located at 667 cm^{-1} can be assigned to C—S stretching vibration from the organic matter in the PDA medium.[29] Its weakened intensity during incubation suggested the fungal consumption of the medium. The peaks at 676, 836, and 1,050 cm^{-1} were assigned to the C—O bending, C—H out of plane bending, and C—O stretching vibrations, respectively.[30,31] These three peaks appeared since Day 3. Then the intensities of these three peaks increased synchronously from Days 3 to 6, which was due to the increased biomass of *A. niger* after a lag period.[19] These peaks (assigned to the organic matters) were active in the IR spectra, whereas many vibrations related to oxalate minerals were not active. Therefore, DRIFT was not able to identify phase of the secondary mineral as the strong signals of the organic matters masked the peaks due to oxalate minerals (see Figure 2).

3.3 | Identification of Pb secondary minerals using RISE

RISE spot analysis successfully identified that secondary Pb minerals with different morphologies (Figure 3). The

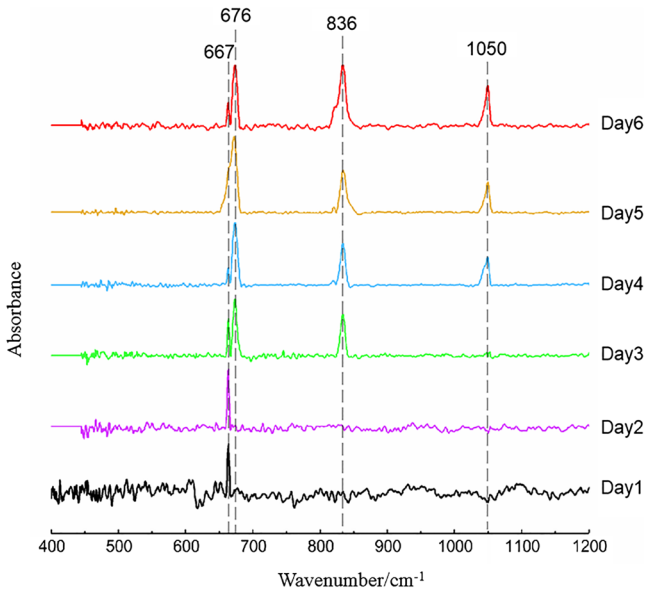

FIGURE 2 DRIFT spectra (400-1200 cm^{-1}) on the surface of Pb foils during 6d incubation with *A. niger*. The spectra were normalized to the intensity of the 667/676 cm^{-1} peak.

smoothing was performed to confirm the appeared peaks in the spectra (see Figures S1 and S2). The peak at 498 cm^{-1} represented the δ_s(O—C—O).[35] Additionally, the ~855 and ~895 cm^{-1} peaks were both assigned to ν_2 (C—C) vibrations. In addition, the spectra displayed peaks at ~1,440, ~1,480, and ~1,590 cm^{-1}, which were assigned to various C—O vibrations of Pb oxalate mineral.[32] Therefore, the characteristic peaks of spot analysis in Figure 3 confirmed that the secondary mineral is Pb oxalate. It should be pointed out that the small (Figure 3a) and large (Figure 3b) Pb oxalate particles demonstrated distinct order (also confirmed after normalization) of the intensities for Raman peaks at ~1,440, ~1,480, and ~1,590 cm^{-1}, suggesting the variable orientation of the secondary Pb mineral (probably due to different growth stage).

A relatively flat surface (Figure 1f) under SEM mode of RISE was applied to conduct Raman mapping. It was confirmed that the secondary minerals preferred to form scale-like morphology (Figure 4a). It was previously proposed that the growth rate of some faces could be inhibited due to the interaction between organic molecules (also secreted from *A. niger*) and metals.[28,33] In this study, (001) face was suppressed due to the fungi creeping on the foils. It indicated that fungi can play a significant role in regulating the process of biocorrosion. The mapping was performed on the basis of six representative peaks, that, 498, 861, 902, 1,447, 1,483, and 1,593 cm^{-1}, respectively. In Raman mapping, the black spots in Figure 4b–g indicated the boundaries within the scaled structure. Moreover, the black area (rather than spots) may be caused by the corrugation of foils.

SEM can observe the morphology of metal surface, but it could not identify secondary substance components or elucidate the degree of the biocorrosion. Instead, Raman spectroscopy can provide information of the secondary substance components and the distribution of them, which demonstrates the full picture of biocorrosion. Therefore it is necessary to combine SEM and Raman spectroscopy to trace the fungi-assisted biocorrosion of metal. RISE is a new technique that can meet these two demands. Our results also clearly demonstrated that Raman is effective to trace the biomineralization of Pb compared with IR. Furthermore, not all the minerals can be identified by Raman, whereas the Raman analysis can effectively identify PbC_2O_4. On the basis of the Raman mapping, the distribution of PbC_2O_4 can be further characterized and examined. Meanwhile, SEM mode of RISE could add the details to further demonstrate metal biocorrosion. Moreover, the RISE technique has no damage to samples, that is, usually considered as a nondestructive technique. The flat surface of metals can promise the RISE analysis in high quality. Although the

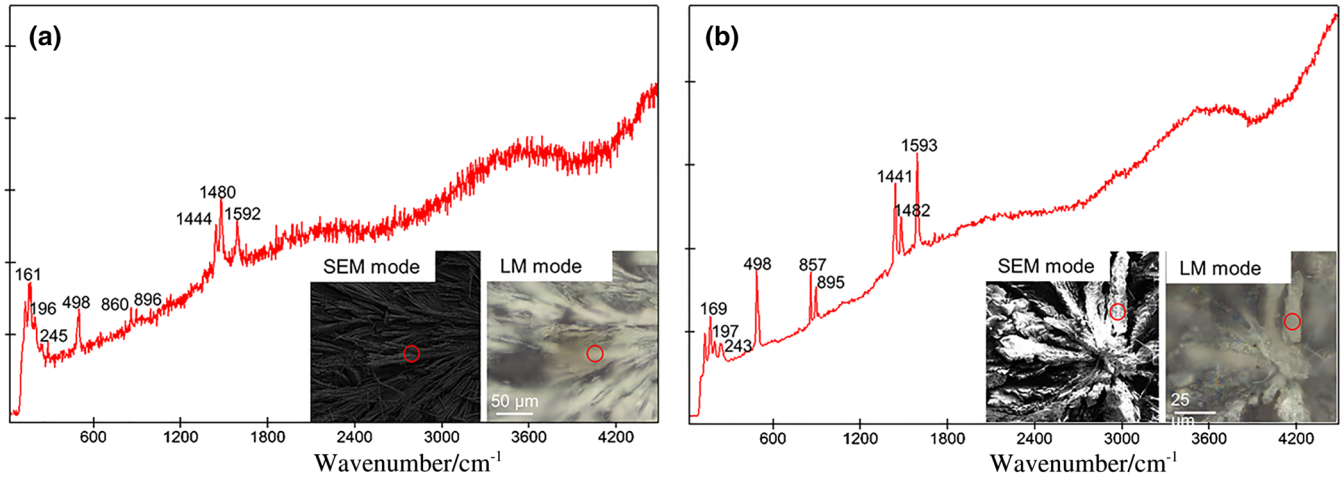

FIGURE 3 RISE spot analysis (0-4500 cm^{-1}) on the secondary Pb-minerals with two different morphologies. A: The area occupied by the small particles as shown in Fig. 1E; B: The area occupied by the large particles as shown in Fig. 1F. The RISE spots were indicated by the circles under both SEM and LM modes.

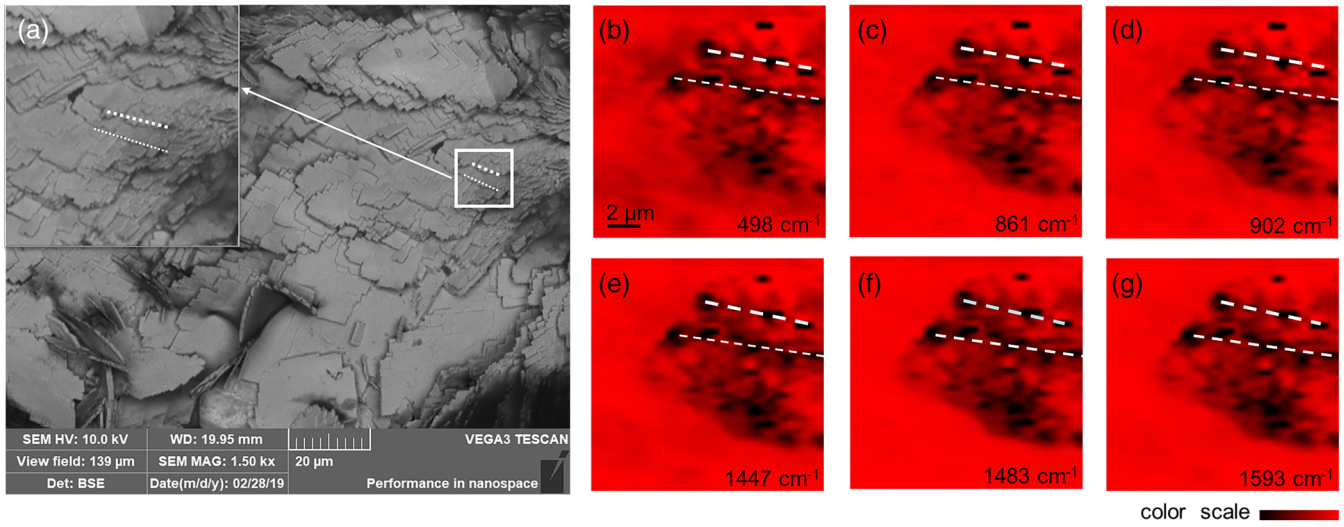

FIGURE 4 RISE analysis on the secondary Pb-minerals with SEM and Raman mapping. A: The image of large particles as shown in Fig. 1F; B-G: The Raman mapping images in characterized peaks of Pb oxalate.

Pb foils is corrugated in our experiment, the images are also clear enough to confirm the appearance of Pb oxalate. Therefore, RISE can provide an efficient approach for the investigation of bioweathering on flat surface of multiple materials.

4 | CONCLUSIONS

In summary, metal and mineral transformations enhanced by microorganisms may result in spoilage of metal materials, biodeterioration of cultural heritage, and acid mine drainage.[34] The biocorrosion of Pb materials hence causes potential environmental risks. It is necessary to clearly trace this process through an effective technique. Fungi play a critical role in metal biocorrosion. SEM can observe the morphology of the mental surface. DRIFT spectra showed the chemical changes on the surface of Pb foils. However, they cannot successfully identify the phases of secondary minerals. Instead, the RISE, combined Raman and SEM, successfully confirmed that the secondary mineral was PbC_2O_4. Furthermore, Raman mapping demonstrates the distribution of PbC_2O_4 architecture. The RISE is hence a powerful technique in tracking biocorrosion of metals.

ACKNOWLEDGEMENTS

This work was supported by National Key R&D Program of China (2017YFC0503902) and the Fundamental Research Funds for the Central Universities

(KYZ201712). This work was also partially supported by Program for Student Innovation Through Research and Training (S20190010 and 201910307090P). We also thank Dr. Juan Li at Nanjing University State Key Laboratory for the SEM analyses. We would like to thank Prof. Lixiang Zhou for the valuable comments on the manuscript.

ORCID

Zhen Li https://orcid.org/0000-0002-2335-3744

REFERENCES

[1] C. P. Rooney, R. G. McLaren, R. J. Cresswell, *Water Air Soil Pollut.* **1999**, *116*, 535.

[2] J. S. Casas, J. Sordo, *Lead* **2006**, *1*, 1.

[3] S. S. Jorgensen, M. Willems, *Ambio* **1987**, *16*, 11.

[4] Y. J. Rhee, S. Hillier, G. M. Gadd, *Curr. Biol.* **2012**, *22*, 237.

[5] Y. J. Rhee, S. Hillier, H. Pendlowski, G. M. Gadd, *Chemosphere* **2014**, *113*, 17.

[6] M. M. Naik, D. Khanolkar, S. K. Dubey, *Lett. Appl. Microbiol.* **2013**, *56*, 99.

[7] R. E. Tatnall *Case Histories*: *Biocorrosion*, **1991**.

[8] G. M. Gadd, *Microbiol-Sgm* **2010**, *156*, 609.

[9] G. M. Gadd, *Elements* **2017**, *13*, 171.

[10] W. P. Iverson, *Adv. Appl. Microbiol.* **1987**, *32*, 1.

[11] S. H. Oliveira, M. A. G. A. Lima, F. P. Franca, M. R. S. Vieira, P. Silva, S. L. Urtiga, *Int. J. Biol. Macromol.* **2016**, *88*, 27.

[12] J. F. Banfield, W. W. Barker, S. A. Welch, A. Taunton, *P. Natl. Acad. Sci. USA* **1999**, *96*, 3404.

[13] H. J. Pel, J. H. de Winde, D. B. Archer, P. S. Dyer, G. Hofmann, P. J. Schaap, G. Turner, R. P. de Vries, R. Albang, *Nat. Biotechnol.* **2007**, *25*, 221.

[14] A. Kapoor, T. Viraraghavan, D. R. Cullimore, *Bioresour. Technol.* **1999**, *70*, 95.

[15] Z. Li, T. Bai, L. Dai, F. Wang, J. Tao, S. Meng, Y. Hu, S. Wang, S. Hu, *Sci. Rep.* **2016**, *6*, 25313.

[16] K. V. Sazanova, S. M. Shchiparev, D. Y. Vlasov, *Microbiology* **2014**, *83*, 516.

[17] R. Young Joon, H. Stephen, G. Geoffrey Michael, *Curr. Biol.* **2012**, *22*, 237.

[18] D. Tian, Z. Q. Jiang, L. Jiang, M. Su, Z. Y. Feng, L. Zhang, S. M. Wang, Z. Li, S. J. Hu, *Environ. Microbiol.* **2019**, *21*, 471.

[19] Z. Li, F. W. Wang, T. S. Bai, J. J. Tao, J. Y. Guo, M. Y. Yang, S. M. Wang, S. J. Hu, *J. Hazard. Mater.* **2016**, *320*, 386.

[20] K. E. Giller, E. Witter, S. P. Mcgrath, *Soil Biol. Biochem.* **2009**, *41*, 2031.

[21] Z. Li, T. S. Bai, L. T. Dai, F. W. Wang, J. J. Tao, S. T. Meng, Y. X. Hu, S. M. Wang, S. J. Hu, *Sci. Rep.* **2016**, *6*, 25313.

[22] N. S. Bolan, R. Naidu, S. Mahimairaja, S. Baskaran, *Biol. Fertil. Soils* **1994**, *18*, 311.

[23] G. Michael, J. Bahri-Esfahani, Q. W. Li, Y. J. Rhee, Z. Wei, M. Fomina, X. J. Liang, *Fungal Biol. Rev.* **2014**, *28*, 36.

[24] D. Purchase, L. N. L. Scholes, D. M. Revitt, R. B. E. Shutes, *J. Appl. Microbiol.* **2009**, *106*, 1163.

[25] M. A. Fomina, I. J. Alexander, J. V. Colpaert, G. M. Gadd, *Soil Biol. Biochem.* **2005**, *37*, 851.

[26] G. M. Gadd, *Mycol. Res.* **2007**, *111*, 3.

[27] J. A. Sayer, G. M. Gadd, *Mycol. Res.* **1997**, *101*, 653.

[28] E. V. Sturm, O. Frank-Kamenetskaya, D. Vlasov, M. Zelenskaya, K. Sazanova, A. Rusakov, R. Kniep, *Am. Mineral.* **2015**, *100*, 2559.

[29] S. K. Nandy, D. K. Mukherjee, S. B. Roy, G. S. Kastha, *Can. J. Chem.* **1973**, *51*, 1139.

[30] J. C. Martinez-Patino, T. A. Lu-Chau, B. Gullon, E. Ruiz, I. Romero, E. Castro, J. M. Lema, *Ind. Crop Prod.* **2018**, *121*, 10.

[31] G. M. Gadd, *Adv. Microb. Physiol.* **1999**, *41*, 47.

[32] N. Mancilla, M. C. D'Antonio, A. C. Gonzalez-Baro, E. J. Baran, *J. Raman Spectrosc.* **2009**, *40*, 2050.

[33] J. G. Yu, H. Tang, B. Cheng, X. J. Zhao, *J. Solid State Chem.* **2004**, *177*, 3368.

[34] G. M. Gadd, X. Pan, *Geomicrobiol. J.* **2016**, *33*, 175.

SUPPORTING INFORMATION

Additional supporting information may be found online in the Supporting Information section at the end of the article.

How to cite this article: Wu Y, Shao X, Jiao H, Song X, He K, Li Z. Tracking the fungus-assisted biocorrosion of lead metal by Raman imaging and scanning electron microscopy technique. *J Raman Spectrosc*. 2020;1–6. https://doi.org/10.1002/jrs.5796